Int. J. Electrochem. Sci., 12 **(2017)** 11479 – 11486, doi: 10.20964/2017.12.70

International Journal of
ELECTROCHEMICAL
SCIENCE
www.electrochemsci.org

Short Communication

Preparation of (MnO_2/RGO)/$Li_7La_3Zr_2O_{12}$/$LiCoO_2$ Solid State Lithium Ion Batteries and Theirs Electrochemical Performance

Hongdong Liu[1,2], Shuyue Yang[2], Rong Hu[2], Haibo Ruan[2], Yongyao Su[2], Lei Zhang[3,], Zhongli Hu[2], Lian Ying Zhang[4,*]*

[1] Faculty of Materials and Energy, Southwest University, Chongqing 400715, P.R. China
[2] Research institute for new materials technology, Chongqing University of Arts and Sciences, Chongqing 402160, PR China
[3] College of life science, Chongqing Normal University, Chongqing 401331, PR China
[4] Institute of Materials for Energy and Environment, College of Materials Science and Engineering, Qingdao University, Qingdao 266071, PR China
[*]E-mail: leizhang0215@126.com, lyzhang@swu.edu.cn

Received: 17 August 2017 / *Accepted:* 11 October 2017 / *Published:* 12 November 2017

Lithium ion batteries (LIBs), also known as energy conversion and storage systems, can provide much greater energy density and power density, and superior cycle life, but they are still limited by the safety issue which arises from their combustible organic electrolytes. Here, a novel all solid state lithium ion batteries (ASSLIBs) have been prepared using $Li_7La_3Zr_2O_{12}$, MnO_2/RGO and $LiCoO_2$ as the solid Li electrolytes, the active anode and cathode material, respectively. A coating method is used for the LIBs preparation. As a result, the novel type LIBs exhibit superior electrochemical performance, impressive cycling stability and better safety. It is indicated that the promising synthetic method used in this work can pave the way for designing safety LIBs with excellent electrochemical performance.

Keywords: Lithium-ion batteries, All solid state, $Li_7La_3Zr_2O_{12}$, Electrochemical performance

1. INTRODUCTION

Lithium ion batteries (LIBs) is an energy storage device characterized as having high energy density and power density, long cycle life and it is of considerable interest in electric vehicles, portable electronics and other high power transportation applications[1-3]. However, conventional LIBs based on the liquid electrolytes suffer from big capacity loss and bad safety due to the electrolyte decomposition and formation of SEI film during the discharge process[4,5]. To overcome this limitation, massive effects have been devoted to find a safety and more superior alternatives to replace the conventional LIBs. The practical use of ASSLIBs have been strongly expected because these batteries have obvious advantages over traditional LIBs in terms of high safety, high energy

density and flexibility, as while as its nonvolatile and nonflammable characters[6,7]. Significantly, owing to the non liquid organic electrolytes, the LIBs can be formed into various shapes, reducing the space and weight, and used as wearable equipment.

Recently the ASSLIBs with inorganic Li-ion conductors which with high lithium-ionic conductivity, good chemical stability and compatibility with electrode materials have attracted attention because of their high energy density, better safety and flexibility. A variety of Li-ion conductors have been investigated including NASICON-structure lithium aluminum germanium phosphate[8], thio-LISICON structure[9], LiOPN[10] and garnet-type $Li_7La_3Zr_2O_{12}$[11,12]. In particular, the composition $Li_7La_3Zr_2O_{12}$ is considered to be one of the most promising materials for ASSLIBs because of its high ionic conductivity, stability against lithium anodes, and large electrochemical window[13]. Our earlier studies [14] show that the $Li_7La_3Zr_2O_{12}$ used as the electrolyte for LIBs displays excellent electrochemical performance and the highest ionic conductivity is 2.11×10^{-4} S cm^{-1}.

Currently the anode electrodes of most commercial LIBs are made of graphite that has low theoretical specific capacity (372 mA h g^{-1}), which is not able to meet the increasing demand especially for high energy and power energy storage systems[1,15]. Therefore, it is urgent to develop new alternative anodes. Nanostructured transition metal oxides (such as Fe_3O_4[16,17], MoO_2[18] and MnO_2[19,20]) are also alternative anodes for LIBs because of their high theoretical specific capacity. Among them, manganese oxide (MnO_2) is a widely used material featuring high theoretical specific capacity (1230 mA h g^{-1}), environmental friendliness and nature abundance[21-23]. Unfortunately, the poor conductivity and high initial capacity loss of MnO_2 restricts seriously its potential applications in LIBs[19,22]. Nowadays, researchers mainly focus on prepared nanostructures of MnO_2 and combining conductive carbon materials (CNTs, graphene) with MnO_2 due to its significant electrochemical properties[24-26]. M. Tour et al. reported that the Graphene-wrapped MnO_2–graphene nanoribbons electrodes can deliver a reversible specific capacity of 890 mAh g^{-1} at 0.1 A g^{-1} after 180 cycles with varying current rates from 0.1 to 1.0 A g^{-1} and increases about 24% compared to the initial capacity after 245 cycles at 0.4 A g^{-1}[22].

In the present work, the ASSLIBs have been prepared by the coating method using $Li_7La_3Zr_2O_{12}$, MnO_2/RGO and $LiCoO_2$ as the solid Li electrolytes, the active anode and cathode material, respectively, and investigate the electrochemical performance. When tested at room temperature, the (MnO_2/RGO) /20μm-$Li_7La_3Zr_2O_{12}$/$LiCoO_2$ batteries achieve 1.87 μAh cm^{-2} of discharge capacity at the first cycle and 0.58 μAh cm^{-2} of capacity after 20 cycles. Meanwhile, the thickness of the electrolyte plays an important role in the performance of the battery. In general, the ASSLIBs demonstrate excellent electrochemical performance, superior cycling stability and better safety.

2. EXPERIMENTAL SECTION

2.1 Preparation of MnO_2/RGO for anode electrode materials

MnO_2/RGO materials were prepared via hydrothermal method as mentioned in our previous papers. Firstly, 18 mg of reduction graphene oxide (RGO) was taken into 30 ml deionized water under

ultrasonic for 30min. Secondly, 0.316 g (2 mmol) of $KMnO_4$ was added to the RGO suspension and stirred at room temperature for 10 minutes. A certain amount of 0.4 mL HCl (3M) was added into mixed solution and stirred for 5 min after $KMnO_4$ completely dissolved. Then the above mixture was transferred into a 50 mL Teflon-lined stainless-steel autoclave and heated at 160 ^oC for 6h. Finally, after cooling to room temperature, the product was centrifuged with deionized water and ethanol, which was followed by drying at 60 °C. The resulting sample was denoted as MnO_2/RGO.

2.2 Preparation of $Li_7La_3Zr_2O_{12}$ Electrolyte

$Li_7La_3Zr_2O_{12}$ was prepared by high temperature solid-state method. The starting materials of $LiOH{\cdot}H_2O$, $La(OH)_3$, ZrO_2 and Al_2O_3 were mixed in the molar ratio of 7.7:3:2:0.15 and milled for 24 in isopropanol in a planetary ball mill with zirconia balls and grinding bowls at 400 rpm min^{-1}. Then the samples were dried at 60 ^oC. Finally, the mixture was sintered at 900 ^oC in air for 12 h (heating and cooling rate: 5 ^oC min^{-1}).

2.3 Preparation of all solid state lithium-ion battery (ASSLIBs)

In our work, the ASSLIBs mode is shown in Fig1. The aluminum foil, copper foil, MnO_2/RGO, $Li_7La_3Zr_2O_{12}$ and $LiCoO_2$ are used as the positive collector, negative collector, negative electrode, electrolyte and positive electrode, respectively. The ASSLIBs prepared in air by the coating method. The positive or negative electrodes were prepared by mixing active materials, acetylene black and PVDF according to the mass ratio of 80:10:10. Then, the electrolyte was prepared from a NMP slurry of the $Li_7La_3Zr_2O_{12}$ and PVDF in the 90:10 weight ratio. The slurry was cast onto the positive or negative working electrodes. Then the positive electrode and negative electrode were pressed together to form a full battery.

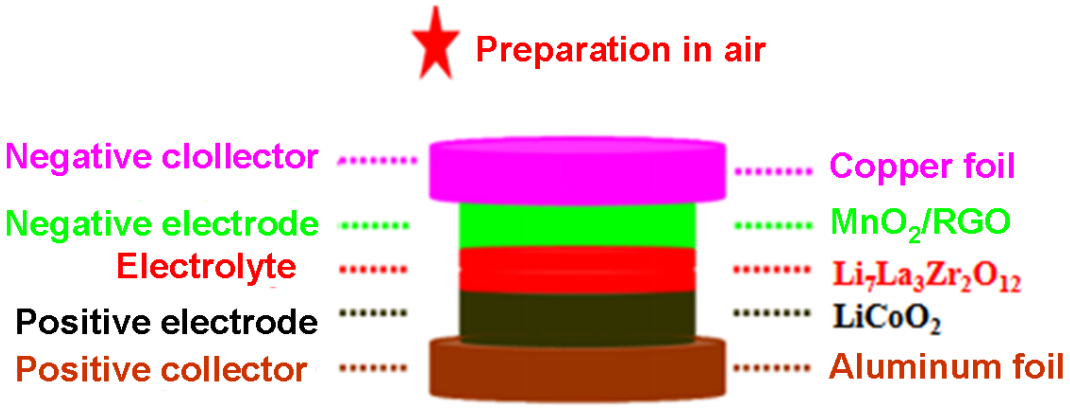

Figure 1. All solid state lithium ion batteries.

In our work, the solid electrolyte thickness were 20 μm, 40 μm, 60 μm, the ASSLIBs were marked as (MnO_2/RGO)/20μm-$Li_7La_3Zr_2O_{12}$/$LiCoO_2$, (MnO_2/RGO)/40μm-$Li_7La_3Zr_2O_{12}$/$LiCoO_2$, (MnO_2/RGO)/60μm-$Li_7La_3Zr_2O_{12}$/$LiCoO_2$.

2.4 Electrochemical performance test

The X-ray powder diffraction (TD-3500X) with Cu Kα radiation operating at 30 kV, 20 mA is usually used to analyze the phase components and crystal structure. The galvanostatic charge and discharge cycling experiments were carried out a Neware battery tester (BTS-610).

3. RESULTS AND DISCUSSION

The electrochemical performance of the ASSLIBs is strongly affected by the thermal and chemical stability between the electrodes and electrolyte. Here, the thermal and chemical stability between the electrodes and electrolyte were examined by X-ray diffraction (XRD) and are shown in Fig.2 and Fig.3. Briefly, the solid electrolyte $Li_7La_3Zr_2O_{12}$ and the working electrode materials (MnO_2/RGO or $LiCoO_2$) were mixed according to the mass ratio of 1:1 and then calcined at 25-200 ^oC for 6h, finally detected the phase composition of the mixture based on XRD measurements.

The X-ray diffraction patterns for the mixture of $Li_7La_3Zr_2O_{12}$ with MnO_2/RGO after heat-treatment are shown in Fig.2. It is observed that all diffraction peaks are well matched with cubic phase $Li_7La_3Zr_2O_{12}$ (JCPDS, 45-0109) and MnO_2 (JCPDS, 44-0141), and do not indicate any additional diffraction lines corresponding to any impurity phases in the temperature range of 25-200 ^oC. Otherwise, the intensity of the diffraction peaks improves with the increase of calcination temperature, indicating that the crystalline of the mixture is gradually increased. Hence, our XRD results prove that the $Li_7La_3Zr_2O_{12}$ and MnO_2 have a better thermal and chemical stability in the temperature range of 25-200 ^oC.

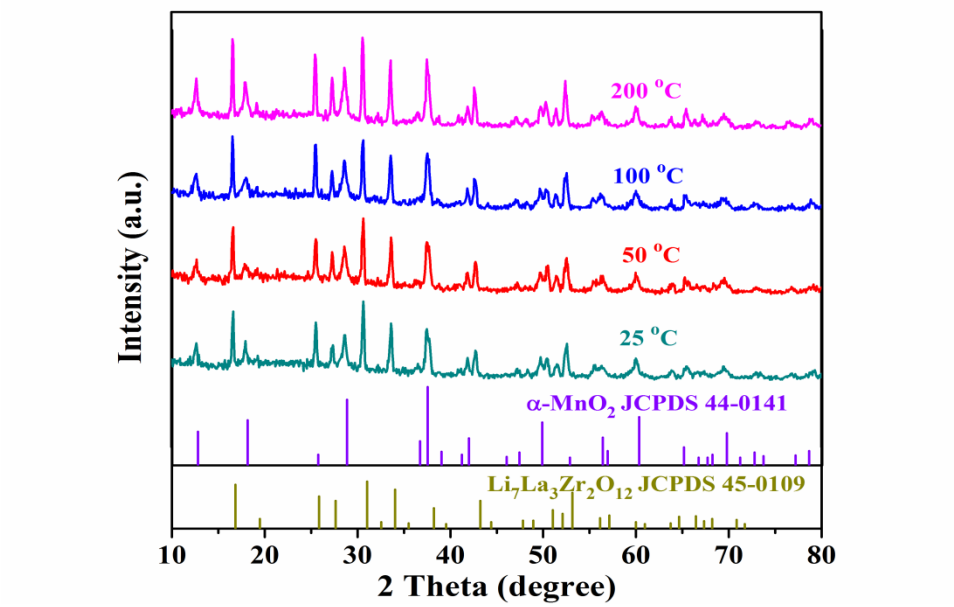

Figure 2. The XRD patterns of the mixture of $Li_7La_3Zr_2O_{12}$ and MnO_2/RGO sintered at different temperature.

The phase compositions of the mixture of $Li_7La_3Zr_2O_{12}$ and $LiCoO_2$ after sintering at different temperatures are shown in Fig.3. The XRD patterns match well with the standard pattern known as a garnet phase $Li_7La_3Zr_2O_{12}$ (PDF 45-0109) and tetragonal phase $LiCoO_2$ (JCPDS, 50-0653). No diffraction peaks belonged to impurity phase is observed. These results suggest that $Li_7La_3Zr_2O_{12}$ and $LiCoO_2$ also have excellent chemical stability ranging from 25 ^oC to 200 ^oC.

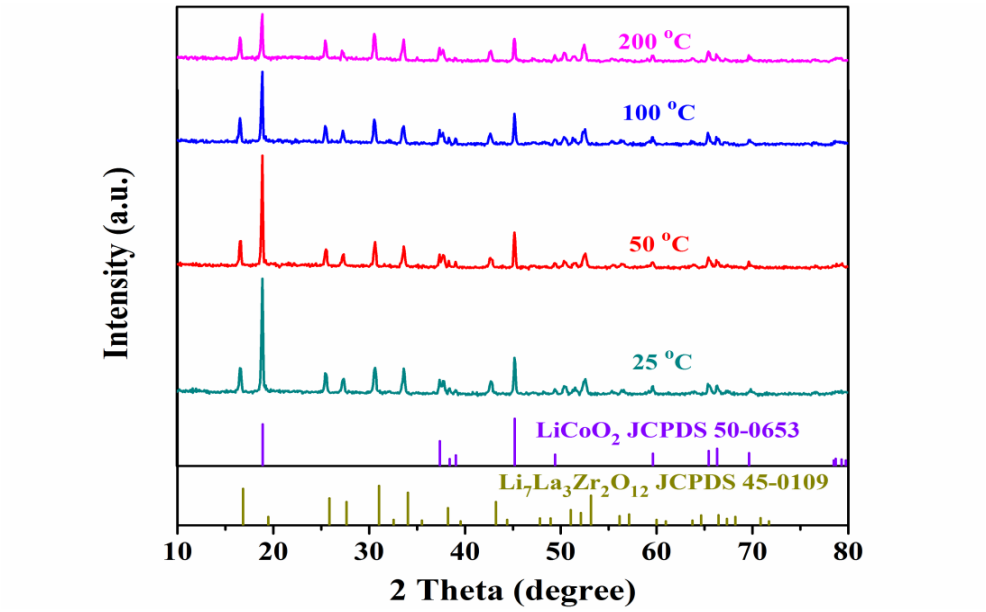

Figure 3. Powder XRD result of the mixture of $Li_7La_3Zr_2O_{12}$ and $LiCoO_2$ sintered at 25-200 ^oC.

The electrochemical performances of $(MnO_2/RGO)/Li_7La_3Zr_2O_{12}/LiCoO_2$ were examined using galvanostatic charge and discharge technologies. The superior cyclic stability of the ASSLIBs is firstly demonstrated under a current density of 2 μA cm^{-2}. As shown in Fig.4, the discharge capacities of (MnO_2/RGO)/20μm-$Li_7La_3Zr_2O_{12}/LiCoO_2$, (MnO_2/RGO)/40μm-$Li_7La_3Zr_2O_{12}/LiCoO_2$, (MnO_2/RGO)/60μm-$Li_7La_3Zr_2O_{12}/LiCoO_2$ are to 1.87 μAh cm^{-2}, 1.60 μAh cm^{-2} and 1.07 μAh cm^{-2} at the first cycle, respectively. According to our previous study[27], it shows that the Li-ion conductivity of $Li_7La_3Zr_2O_{12}$ is 2.11×10^{-4} S cm^{-1} at 25 °C, much higher than 3.5×10^{-6} S cm^{-1} of Li_2O-B_2O_3-P_2O_5[28],1.8×10^{-4} S cm^{-1} of Li_2S-GeS_2[29], 6.4×10^{-6} S cm^{-1} of LiPON[30], and 2.46×10^{-5} S cm^{-1} of $Li_{1+x}MxTi_{2-x}(PO4)_3$[31] in table 1, so the first discharge capacity of(MnO_2/RGO)/20μm-$Li_7La_3Zr_2O_{12}/LiCoO_2$ is higher than previous reports[32,33] from table 2. The results shows that the electrochemical capacity increases with the decrease of the thickness of the inorganic solid electrolyte. Then the second discharge capacities are sharply dropped. The high irreversible capacity losses of the three batteries are probably associated with the charge transfer and interfacial resistance. Starting from the second cycle, the reversible capacity of (MnO_2/RGO)/20μm-$Li_7La_3Zr_2O_{12}/LiCoO_2$, (MnO_2/RGO)/40μm-$Li_7La_3Zr_2O_{12}/LiCoO_2$, (MnO_2/RGO)/60μm-$Li_7La_3Zr_2O_{12}/LiCoO_2$ gradually decreases to 0.58 μAh cm^{-2}, 0.41 μAh μcm^{-2} and 0.24 μAh cm^{-2} after 20 cycles, respectively.The capacity attenuation rates of the 20 cycles are 3.6%, 3.9% and 4.1%, respectively.As the thickness of

the inorganic solid electrolyte increases, the capacity attenuation is greater. It is noteworthy that the cycling performance of (MnO_2/RGO)/20μm-$Li_7La_3Zr_2O_{12}$/$LiCoO_2$ is superior to that of (MnO_2/RGO)/40μm-$Li_7La_3Zr_2O_{12}$/$LiCoO_2$ and (MnO_2/RGO)/60μm-$Li_7La_3Zr_2O_{12}$/$LiCoO_2$. The increasing trend of the capacity of ASSLIBs with the electrolyte thickness decreases is likely due to the lower charge transfer and interfacial resistance.

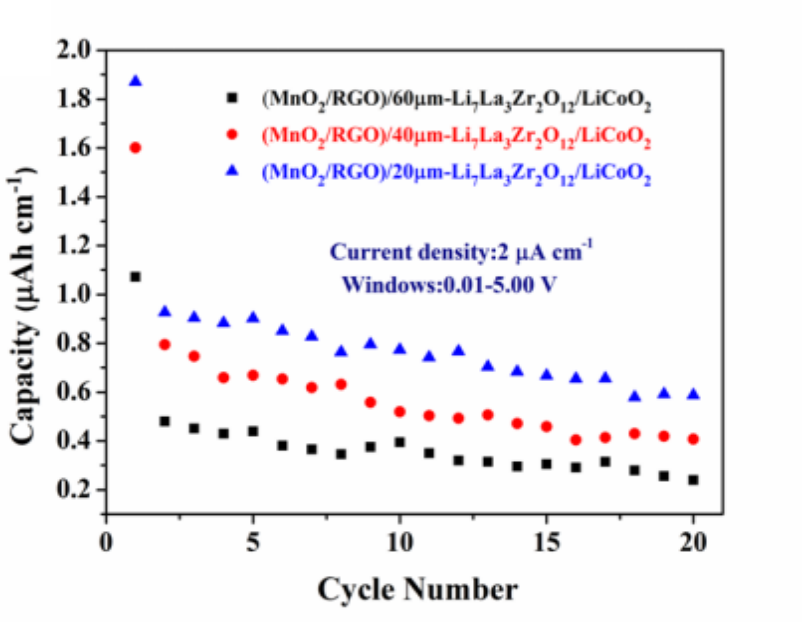

Figure 4. Comparative cycling performance of (MnO_2/RGO)/20μm-$Li_7La_3Zr_2O_{12}$/$LiCoO_2$, (MnO_2/RGO)/40μm-$Li_7La_3Zr_2O_{12}$/$LiCoO_2$, (MnO_2/RGO)/60μm-$Li_7La_3Zr_2O_{12}$/$LiCoO_2$ at a current density of 2 μA cm^{-2}.

Table 1. The ionic conductivity of different inorganic solid electrolytes

Inorganic solid electrolyte	Li-ion conductivity/ S.cm^{-1}	References
$Li_7La_3Zr_2O_{12}$	2.11×10^{-4}	This work
Li_2O-B_2O_3-P_2O_5	3.5×10^{-6}	[28]
Li_2S-GeS_2	1.8×10^{-4}	[29]
LiPON	6.4×10^{-6}	[30]
$Li_{1+x}MxTi_{2-x}(PO_4)_3$	2.46×10^{-5}	[31]

Table 2. The first discharge capacity of different kind of solid state lithium ion batteries

Solid state lithium ion batteries	First discharge capacity/μAh cm^{-2}	References
(MnO_2/RGO)/20μm-$Li_7La_3Zr_2O_{12}$/$LiCoO_2$	1.87	This work
$LiMn_2O_4$/ Li_2O-V_2O_5-SiO_2/SnO	1.5	[32]
Li-Mn-O(Amorphous)/ Li_2O-Al_2O_3-TiO_2-P_2O_5/Cu	0.25	[33]

The rate capability of (MnO_2/RGO)/20μm-$Li_7La_3Zr_2O_{12}$/$LiCoO_2$ was examined (Fig. 5). The stable discharge–charge capacity of 0.922, 0.392 and 0.106 μAh cm^{-2} can be delivered at varied

currents of 2, 5 and 10 μA cm^{-2}, respectively. After the current density was 2 μA cm^{-2}, the cell capacity can recover to 0.249 μAh cm^{-2}. Obviously, the (MnO_2/RGO)/20μm-$Li_7La_3Zr_2O_{12}$/$LiCoO_2$ battery has better capacity retention.

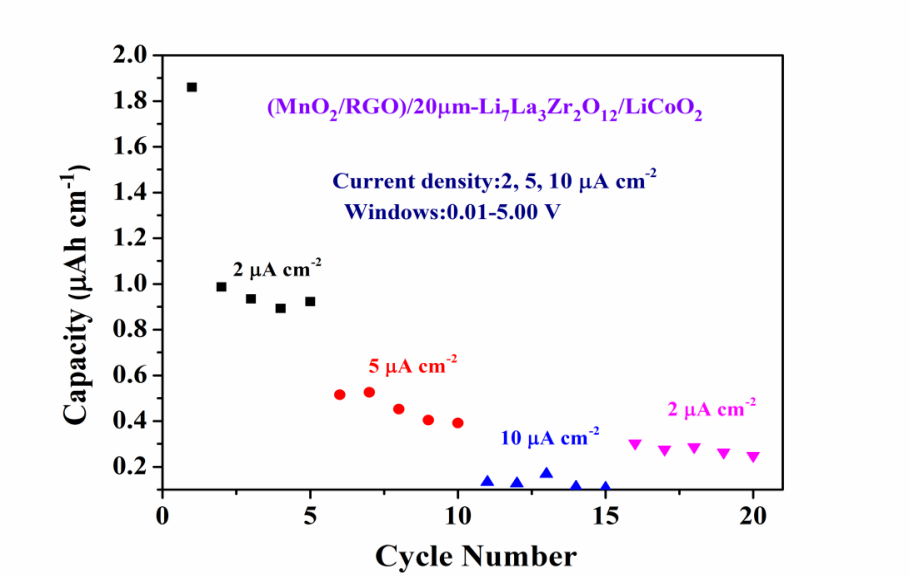

Figure 5. The rate performance of (MnO_2/RGO)/20μm-$Li_7La_3Zr_2O_{12}$/$LiCoO_2$ battery at different current densities.

4. CONCLUSIONS

In summary, the (MnO_2/RGO)/20μm-$Li_7La_3Zr_2O_{12}$/$LiCoO_2$, (MnO_2/RGO)/40μm-$Li_7La_3Zr_2O_{12}$/$LiCoO_2$, (MnO_2/RGO)/60μm-$Li_7La_3Zr_2O_{12}$/$LiCoO_2$ batteries were successfully fabricated by controlling the thickness of the solid electrolyte ($Li_7La_3Zr_2O_{12}$) via the coating method. As a consequence, superior cycling performance (1.87 μAh cm^{-2} at 2 μA cm^{-2} for first cycle, 0.58μAh cm^{-2} over 20 cycles) and excellent rate capability (0.106 μAh cm^{-2} at 10 μA cm^{-2}) were achieved. Furthermore, the electrochemical performance of the batteries increased with decreasing the thickness of the $Li_7La_3Zr_2O_{12}$. Such a simple and scalable route to construct ASSLIBs may be further extended to other electrochemical energy storage applications.

ACKNOWLEDGEMENTS
This work was financially supported by Basic and Frontier Research Program of Chongqing Municipality (cstc2015jcyjA90020) and (cstc2017jcyjAX0326), China Postdoctoral Science Foundation (2015M582499) and Postdoctoral special Foundation of Chongqing (Xm2015064).

References

1. X. Fan, J. Shao, X. Xiao, L. Chen, X. Wang, S. Li, H. Ge, *Journal of Materials Chemistry* A, 2 (2014) 14641.
2. Y. Xu, Z. Lin, X. Zhong, B. Papandrea, Y. Huang, X. Duan, *Angewandte Chemie*, 54 (2015) 5345.
3. S. Fang, L. Shen, G. Xu, P. Nie, J. Wang, H. Dou, X. Zhang, *Acs Applied Materials & Interfaces*, 6

(2014) 6497.
4. C. Bernuy-Lopez, W. Manalastas, J. M. Lopez del Amo, A. Aguadero, F. Aguesse, J. A. Kilner, *Chemistry of Materials*, 26 (2014) 3610.
5. K. Takada, Acta Materialia, 61 (2013) 759.
6. L. Dhivya, R. Murugan, *Acs Applied Materials & Interfaces*, 6 (2014) 17606.
7. A. Ramzy, V. Thangadurai, *ACS Applied Materials & Interfaces*, 2 (2010) 385.
8. P. Zhang, M. Matsui, A. Hirano, Y. Takeda, O. Yamamoto, N. Imanishi, *Solid State Ionics*, 253 (2013) 175.
9. Y. Wang, Z. Liu, X. Zhu, Y. Tang, F. Huang, *Journal of Power Sources*, 224 (2013) 225.
10. G. Li, M. Li, L. Dong, X. Li, D. Li, *International Journal of Hydrogen Energy,* 39 (2014) 17466.
11. M. Zhang, Z. Huang, J. Cheng, O. Yamamoto, N. Imanishi, B. Chi, J. Pu, J. Li, *Journal of Alloys and Compounds*, 590 (2014) 147.
12. S. Narayanan, F. Ramezanipour, V. Thangadurai, *The Journal of Physical Chemistry* C, 116 (2012) 20154.
13. Y. Cao, Y.-Q. Li, X.-X. Guo, *Chinese Physics* B, 22 (2013) 559.
14. Z. Hu, H. Liu, H. Ruan, R. Hu, Y. Su, L. Zhang, *Ceramics International*, 42 (2016) 12156.
15. L. Yin, Z. Zhang, Z. Li, F. Hao, Q. Li, C. Wang, R. Fan, Y. Qi, *Advanced Functional Materials*, 24 (2014) 4176.
16. W. Wei, S. Yang, H. Zhou, I. Lieberwirth, X. Feng, K. Muellen, *Advanced Materials*, 25 (2013) 2909.
17. L.Y. Zhang, W. Zhang, Z. Zhou, C.M. Li, *Journal of Colloid and Interface Science*, 476 (2016) 200.
18. B. Guo, X. Fang, B. Li, Y. Shi, C. Ouyang, Y.-S. Hu, Z. Wang, G. D. Stucky, L. Chen, *Chemistry of Materials*, 24 (2012) 457.
19. L. Xing, C. Cui, C. Ma, X. Xue, *Materials Letters*, 65 (2011) 2104.
20. H. Liu, Z. Hu, Y. Su, H. Ruan, R. Hu, L. Zhang, *Applied Surface Science*, 392 (2017) 777.
21. X. Li, Y. Zhang, Q. Zhong, T. Li, H. Li, J. Huang, *Applied Surface Science*, 313 (2014) 877.
22. L. Li, A.-R. O. Raji, J. M. Tour, *Advanced Materials*, 25 (2013) 6298.
23. H. Liu, Z. Hu, L. Tian, Y. Su, H. Ruan, L. Zhang, R. Hu, *Ceramics International*, 42 (2016) 13519.
24. L. Peng, X. Peng, B. Liu, C. Wu, Y. Xie, G. Yu, *Nano Letters*, 13 (2013) 2151.
25. S. Wu, W. Chen, L. Yan, *Journal of Materials Chemistry* A, 2 (2014) 2765.
26. Y. Liu, D. He, J. Duan, Y. Wang, S. Li, *Materials Chemistry and Physics*, 147 (2014) 141.
27. Z. Hu, H. Liu, H. Ruan, R. Hu, Y. Su, L. Zhang, *Ceramics International*, 42 (2016) 12156.
28. F. Wu, Y. Zheng, L. Li, G. Tan, R. Chen, S. Chen, *Journal of Physical Chemistry C*, 117 (2013) 19280.
29. Y. Ito, A. Sakuda, T. Ohtomo, A. Hayashi, M. Tatsumisago, *Solid State Ionics*, 236 (2013) 1.
30. N. Suzuki, S. Shirai, N. Takahashi, T. Inaba, T. Shiga, *Solid State Ionics*, 191 (2011) 49.
31. H. Chen, H. Tao, X. Zhao, Q. Wu, *Journal of Non-Crystalline Solids*, 357 (2011) 3267.
32. Y. Iriyama, C. Yada, T. Abe, Z. Ogumi, K. Kikuchi, *Electrochemistry Communications*, 8 (2006) 1287.
33. N. Kuwata, R. Kumar, K. Toribami, T. Suzuki, T. Hattori, J. Kawamura, *Solid State Ionics*, 177 (2006) 2827.